Journal of Clinical and Translational Hepatology **2024**
DOI: 10.14218/JCTH.2024.00197

Original Article

SOX9 Overexpression Ameliorates Metabolic Dysfunction-associated Steatohepatitis Through Activation of the AMPK Pathway

Juan Deng[1#], Kai Ding[2#], Shuqing Liu[2], Fei Chen[2], Ru Huang[2], Bonan Xu[2], Xin Zhang[2*] and Weifen Xie[1,2,3*]

[1]Department of Gastroenterology, Shanghai East Hospital, School of Medicine, Tongji University, Shanghai, China; [2]Department of Gastroenterology, Changzheng Hospital, Naval Medical University, Shanghai, China; [3]Shanghai Institute of Stem Cell Research and Clinical Translation, Shanghai, China

Received: June 14, 2024 | **Revised:** December 03, 2024 | **Accepted:** December 04, 2024 | **Published online:** December 20, 2024

Abstract

Background and Aims: The transcription factor sex-determining region Y-related high-mobility group-box gene 9 (SOX9) plays a critical role in organ development. Although SOX9 has been implicated in regulating lipid metabolism *in vitro*, its specific role in metabolic dysfunction-associated steatohepatitis (MASH) remains poorly understood. This study aimed to investigate the role of SOX9 in MASH pathogenesis and explored the underlying mechanisms. ***Methods:*** MASH models were established using mice fed either a methionine- and choline-deficient (MCD) diet or a high-fat, high-fructose diet. To evaluate the effects of SOX9, hepatocyte-specific SOX9 deletion or overexpression was performed. Lipidomic analyses were conducted to assess how SOX9 influences hepatic lipid metabolism. RNA sequencing was employed to identify pathways modulated by SOX9 during MASH progression. To elucidate the mechanism further, HepG2 cells were treated with an adenosine monophosphate-activated protein kinase (AMPK) inhibitor to test whether SOX9 acts via AMPK activation. ***Results:*** SOX9 expression was significantly elevated in hepatocytes of MASH mice. Hepatocyte-specific SOX9 deletion exacerbated MCD-induced MASH, whereas overexpression of SOX9 mitigated high-fat, high-fructose-induced MASH. Lipidomic and RNA sequencing analyses revealed that SOX9 suppresses the expression of genes associated with lipid metabolism, inflammation, and fibrosis in MCD-fed mice. Furthermore, SOX9 deletion inhibited AMPK pathway activation, while SOX9 overexpression enhanced it. Notably, administration of an AMPK inhibitor negated the protective effects of SOX9 overexpression, leading to increased lipid accumulation in HepG2 cells. ***Conclusions:*** Our findings demonstrate that SOX9 overexpression alleviates hepatic lipid accumulation in MASH by activating the AMPK pathway. These results highlight SOX9 as a promising therapeutic target for treating MASH.

Citation of this article: Deng J, Ding K, Liu S, Chen F, Huang R, Xu B, *et al*. SOX9 Overexpression Ameliorates Metabolic Dysfunction-associated Steatohepatitis Through Activation of the AMPK Pathway. J Clin Transl Hepatol 2024. doi: 10.14218/JCTH.2024.00197.

Introduction

The prevalence of metabolic dysfunction–associated steatotic liver disease (MASLD), previously referred to as nonalcoholic fatty liver disease, has risen sharply alongside increasing rates of metabolic syndrome, diabetes, and obesity.[1] MASLD can progress to metabolic dysfunction–associated steatohepatitis (MASH), a condition that may lead to liver cirrhosis and hepatocellular carcinoma.[2] Currently, MASLD affects approximately 25% of adults worldwide, making it the leading cause of liver-related morbidity and mortality.[3] Despite its widespread prevalence and growing impact on public health, there are currently no effective treatments for MASLD.[4]

The transcription factor sex-determining region Y-related high mobility group-box gene 9 (SOX9) plays a crucial role in the development of multiple organs, including the bones, heart, testes, pancreas, lungs, intestines, and nervous system.[5] In the liver, SOX9 is highly expressed in bile duct cells under normal conditions, with lower levels observed in a subset of periportal hepatocytes.[6] During pathological states, SOX9 expression increases in response to liver injury and hepatocellular carcinoma.[7,8] SOX9-positive hepatocytes play an essential role in restoring liver mass during regeneration.[7] Furthermore, SOX9 supports the proliferation, self-renewal, and tumorigenic capacity of liver cancer stem cells, contributing to hepatocellular carcinoma progression.[9]

Previous studies have demonstrated that SOX9 regulates lipid metabolism in mesenchymal and skeletal progenitor cells.[10,11] Dysregulated lipid metabolism is a key driver of MASH progression. However, the role of SOX9 in MASH remains poorly understood. Given the critical link between lipid metabolism and liver pathology, we hypothesize that SOX9

Keywords: Sex-determining region Y-related high-mobility group-box gene 9; SOX9; Metabolic dysfunction-associated steatohepatitis; MASH; Adenosine monophosphate-activated protein kinase; AMPK; Lipid accumulation.

[#]Contributed equally to this work.

[*]**Correspondence to:** Weifen Xie, Department of Gastroenterology, Shanghai East Hospital, School of Medicine, Tongji University, Shanghai 200092, China; Department of Gastroenterology, Changzheng Hospital, 415 Fengyang Road, Shanghai 200003, China. ORCID: https://orcid.org/0000-0002-7137-112X. Tel: +86-21-8188-5341, Fax: +86-21-8188-9624, E-mail: weifenxie@smmu.edu.cn; Xin Zhang, Department of Gastroenterology, Changzheng Hospital, Naval Medical University, 415 Fengyang Road, Shanghai 200003, China. ORCID: https://orcid.org/0000-0001-5712-6614. Tel: +86-21-8188-5341, Fax: +86-21-8188-9624, E-mail: zhang68@hotmail.com.

influences lipid metabolism in hepatocytes, thereby affecting the development and progression of MASH.

Adenosine monophosphate-activated protein kinase (AMPK) serves as a key metabolic regulator, balancing cellular energy expenditure and storage.[12] It enhances glucose and lipid catabolism, inhibits protein synthesis, and increases ATP levels to maintain energy homeostasis.[13] Studies consistently show that activating AMPK signaling alleviates MASH, while its inhibition worsens the condition, underscoring AMPK as a promising therapeutic target for MASH.[14–17] For instance, liver-specific AMPK activation in genetically modified mice suppresses MASLD induced by a high-fat diet,[17] whereas hepatic AMPK knockout exacerbates MASH caused by a choline-deficient high-fat diet.[16] These findings highlight the protective role of AMPK activation in MASH. However, it remains unclear whether SOX9 directly regulates the AMPK pathway.

In this study, we observed a significant increase in SOX9 expression in hepatocytes under lipotoxic conditions. Functionally, SOX9 reduced hepatic steatosis, inflammation, and fibrogenesis in methionine- and choline-deficient (MCD) diet-induced MASH. Additionally, hepatocyte-specific SOX9 overexpression alleviated steatohepatitis caused by a high-fat, high-fructose (HFF) diet. Mechanistic analyses revealed that SOX9 promotes AMPK pathway activation. Collectively, these findings position SOX9 as a potential therapeutic target for MASH intervention.

Methods

Animals

MASH was induced using either the MCD or HFF diet. In the MCD model, mice were provided ad libitum access to either the MCD diet (TP 3005M) or a standard control diet (TP 3005 GS), both supplied by Trophic Animal Feed High-tech Company, China, for six to eight weeks. For the HFF model, mice were fed a Western diet (14% protein, 42% fat, 44% carbohydrates, and 0.2% cholesterol; TP 26304; TrophicDiet, Nantong, China) and given a carbohydrate-enriched drinking solution containing 42 g/L of total carbohydrates (55% fructose and 45% sucrose by weight). Animals in the HFF group had unrestricted access to this diet for 12 weeks.

SOX9$^{f/f}$ mice were obtained from Jackson Laboratory (Bar Harbor, ME, USA). To achieve hepatocyte-specific SOX9 knockout (*SOX9*^{HKO}), six-week-old *SOX9*$^{f/f}$ mice received a single tail-vein injection of AAV8-TBG-Cre at a dose of 2×10^{11} genome copies. Control mice were injected with an equivalent dose of AAV8-TBG (control virus). Two weeks after viral injection, mice in the *SOX9*^{HKO} and control groups were fed the MCD diet for six weeks.

We used six-week-old male C57BL/six mice, obtained from Shanghai Slac Laboratory Animal Co., Ltd. (Shanghai, China), to investigate the effects of SOX9 overexpression. For hepatocyte-specific overexpression of SOX9, mice received a single tail-vein injection of AAV8-TBG-*SOX9* (AAV-*SOX9*) at a dose of 4×10^{11} genome copies. After two weeks, the mice were fed the MCD diet for eight weeks. Control mice were injected with AAV8-TBG-GFP (control virus) at an equivalent dose and volume.

In a separate experiment, six-week-old male C57BL/six mice were fed the HFF diet for six weeks to induce steatohepatitis. Following this period, the mice received a single tail-vein injection of either AAV-GFP or AAV-*SOX9* at a dose of 4×10^{11} genome copies. After injection, the animals continued the HFF diet for an additional six weeks.

Before the experiments, all mice were acclimated for one week in a temperature-controlled environment (25 ± 3 °C) with a 12-h light/12-h dark cycle to ensure uniform conditions.

Human liver samples

Liver samples were collected from patients with suspected MASLD undergoing hepatic surgery for conditions such as liver hemangioma or hepatic cysts at the Eastern Hepatobiliary Surgery Hospital in Shanghai, China. All participants provided written informed consent prior to sample collection.

Cell culture

HepG2 cells were maintained in DMEM supplemented with 10% FBS at 37 °C in a 5% CO_2 incubator. To model cellular steatosis *in vitro*, HepG2 cells were treated for 24 h with a mixture of palmitic acid (0.5 mM) and oleic acid (1 mM), collectively referred to as PO, dissolved in 0.5% fatty acid-free bovine serum albumin (BSA). Control cells received only 0.5% fatty acid-free BSA. To inhibit AMPK activation, HepG2 cells were exposed to Compound C (S7306, Selleck) at a concentration of 10 μM.

Virus and small interfering RNA (siRNA)

Recombinant adenoviruses, adenovirus (Ad)-SOX9 and Ad-GFP, were generated as described previously.[18] siRNA targeting SOX9 and the corresponding negative control were obtained from GenePharma.

Quantitative real-time polymerase chain reaction (qRT-PCR)

Total RNA was extracted from liver tissues using TRIzol Reagent.[19] qRT-PCR was performed using a SYBR Green PCR Kit.[20] Expression levels were normalized to β-actin, which served as the internal control. The primer sequences used in the analyses are provided in Supplementary Table 1.

Western blotting

Cells or liver tissues were lysed in buffer supplemented with PMSF protease inhibitor, and proteins were separated using SDS-PAGE. The proteins were then transferred onto nitrocellulose membranes.[21] After blocking with PBST containing 5% skim milk, the membranes were incubated overnight at 4°C with primary antibodies. Subsequently, they were probed with secondary antibodies for 1 h. Protein signals were visualized using an Odyssey infrared imaging system at wavelengths of 700 or 800 nm. Details of the primary antibodies used are provided in Supplementary Table 2.

RNA-sequencing (RNA-seq) and bioinformatics analysis

RNA-seq and bioinformatics analyses followed established protocols.[22] Briefly, RNA extracted from mouse liver tissue was sequenced using the Illumina HiSeq platform. RNA library preparation was performed with the TruSeq® RNA Sample Preparation Kit, and library construction and sequencing were conducted by the Shanghai Biotechnology Corporation. Differentially expressed genes (DEGs) were identified using DESeq2, and enrichment analysis for Gene Ontology categories was performed with Fisher's exact test. Additionally, Gene Set Enrichment Analysis was used to assess pathway enrichment. The RNA-seq dataset has been deposited in the NCBI Gene Expression Omnibus under accession number GSE237075.

Lipidomic analysis

Liver samples were processed, and lipids were detected following established protocols.[23] Lipidomic analysis was car-

ried out using the Majorbio Cloud Platform (https://cloud.majorbio.com). Data preprocessing aimed to reduce variability, which involved filling missing values with the mean, normalizing the dataset, and performing quality control to ensure that the relative standard deviation of ions in the quality control samples remained below 30%. Log10 transformation was applied to correct for heteroscedasticity. Differential metabolite analysis was performed using the following criteria: a *p*-value less than 0.05, a variable importance in projection value greater than 1, and a fold change exceeding 1. The analysis was based on orthogonal partial least squares discriminant analysis and an unpaired Student's *t*-test.

Histological, immunohistochemical, and immunofluorescence analyses

Liver tissues were fixed in formalin and paraformaldehyde, then processed into paraffin and frozen sections. Hematoxylin-eosin staining was used for general morphological analysis, Oil Red O staining for steatosis assessment, and Sirius Red staining for collagen deposition. Histological evaluation employed the nonalcoholic fatty liver disease activity score, derived from the semiquantitative Nonalcoholic Steatohepatitis Clinical Research Network scoring system.[24] The extent of steatosis and fibrosis was quantified by measuring areas stained with Oil Red O and Sirius Red, respectively. ImageJ software was used for quantification by converting images to grayscale, applying thresholding, and measuring both positive and total areas.[25] Immunohistochemistry was performed on 4-μm paraffin-embedded liver sections, analyzed using a photomicroscope. Immunofluorescence staining was carried out using a TCS SP8 confocal microscope (Leica, Wetzlar, Germany).[26] Detailed information on primary antibodies is provided in Supplementary Table 2.

Assessment of serum biochemical parameters

Serum samples from mice were analyzed for liver function markers. Levels of alanine transaminase (ALT), aspartate aminotransferase (AST), and total bilirubin (TBIL) were measured using commercial detection kits (ALT: 992-63991, AST: 998-62191, TBIL: 996-16401) from Wako Pure Chemical Industries, Chuo-ku, Osaka, Japan.

Cellular Nile Red staining

HepG2 cells were fixed with 4% paraformaldehyde and stained with 1 mg/mL Nile Red (HY-D0718, MCE) to assess intracellular lipid accumulation.[27]

Public data source

Transcriptomic data from MASLD and control liver samples were retrieved from the Gene Expression Omnibus, under accession ID GSE135251. RNA sequencing data were analyzed using the ggplot2 package in R and are presented in Fragments Per Kilobase of transcript per Million mapped reads format.

Statistics

All statistical analyses were performed using GraphPad Prism software. Data are presented as mean ± SEM. Comparisons between two groups were conducted using an unpaired two-tailed Student's *t*-test. Statistical significance was defined as $p < 0.05$.

Results

SOX9 suppresses PO-induced lipid accumulation

To investigate the role of SOX9 in MASH, we analyzed publicly available transcriptomic data from 206 liver samples of MASH patients and 10 controls (GSE135251). Our analysis revealed significantly elevated SOX9 expression in the liver tissues of MASH patients (Supplementary Fig. 1A). To further assess SOX9 expression in hepatocytes during MASH progression, we performed immunohistochemical staining on liver tissues from patients with normal livers and MASH (Supplementary Fig. 1B) and from control mice and mice with MCD- or HFF-induced MASH (Fig. 1A and B). These results confirmed increased SOX9 expression in hepatocytes of both MASH patients and mice, suggesting a potential role for SOX9 in hepatocellular lipid metabolism. Next, we examined the impact of SOX9 on lipotoxicity in hepatocytes. HepG2 cells were transduced with either Ad-SOX9 or Ad-GFP and subsequently treated with PO (Fig. 1C). Quantitative real-time PCR revealed that SOX9 overexpression significantly reduced mRNA levels of genes involved in de novo lipogenesis (DNL) (fatty acid synthase, sterol regulatory element-binding protein 1, and acetyl-CoA carboxylase 1) and lipid transport (fatty acid binding protein 1 and cluster of differentiation 36) in both HepG2 and AML12 cells (Fig. 1D, Supplementary Fig. 2A and B). Nile Red staining further demonstrated that SOX9 overexpression markedly reduced PO-induced lipid accumulation in HepG2 cells (Fig. 1E). To complement these findings, we designed two siRNAs targeting SOX9 (siSOX9-1 and siSOX9-2) to knock down SOX9 expression (Fig. 1F). SOX9 knockdown resulted in increased expression of genes associated with DNL and lipid transport (Fig. 1G) and exacerbated PO-induced lipid accumulation (Fig. 1H). Together, these results suggest that SOX9 suppresses lipid accumulation induced by lipotoxicity.

SOX9 attenuates MCD-induced MASH

To examine the role of hepatocyte SOX9 in MASH, we generated $SOX9^{HKO}$ mice by administering AAV8-TBG-Cre via tail vein injection into $SOX9^{f/f}$ mice (Fig. 2A). $SOX9^{HKO}$ and littermate $SOX9^{f/f}$ mice were fed an MCD diet for six weeks. Immunohistochemical staining and western blotting confirmed SOX9 depletion in hepatocytes of $SOX9^{HKO}$ mice (Fig. 2B and C). Histological analyses, including hematoxylin-eosin, Oil Red O, and Sirius Red staining, revealed increased steatosis, lipid accumulation, and fibrosis in $SOX9^{HKO}$ mice following MCD feeding (Fig. 2D and E). Consistently, $SOX9^{HKO}$ mice showed significantly elevated expression of genes involved in DNL (fatty acid synthase, sterol regulatory element-binding protein 1, and acetyl-CoA carboxylase 1) and lipid transport (cluster of differentiation 36 and fatty acid binding protein 1) but no significant changes in genes related to fatty acid oxidation (peroxisome proliferator-activated receptor alpha, carnitine palmitoyltransferase 1, and carnitine palmitoyltransferase 2) compared to $SOX9^{f/f}$ mice (Fig. 2F). Additionally, SOX9 depletion was associated with upregulated expression of inflammation-related (C-C motif chemokine ligand 2 and interleukin 6) and fibrosis-related genes (collagen type I alpha 1 and actin alpha 2) (Fig. 2F). Serum levels of ALT, AST, and TBIL were significantly higher in $SOX9^{HKO}$ mice than in $SOX9^{f/f}$ controls after MCD feeding (Fig. 2G). These findings indicate that the absence of SOX9 exacerbates MCD-induced MASH.

To further assess the impact of SOX9 on hepatic steatosis, we overexpressed SOX9 by injecting AAV-*SOX9* or AAV-GFP into six-week-old male mice, followed by an eight-week MCD diet (Supplementary Fig. 3A). Liver tissues from AAV-*SOX9*-treated mice showed significantly increased SOX9 expression compared to controls (Supplementary Fig. 3B and C). SOX9 overexpression mitigated steatosis, lipid accumulation, and fibrosis (Supplementary Fig. 3D and E). Additionally, SOX9

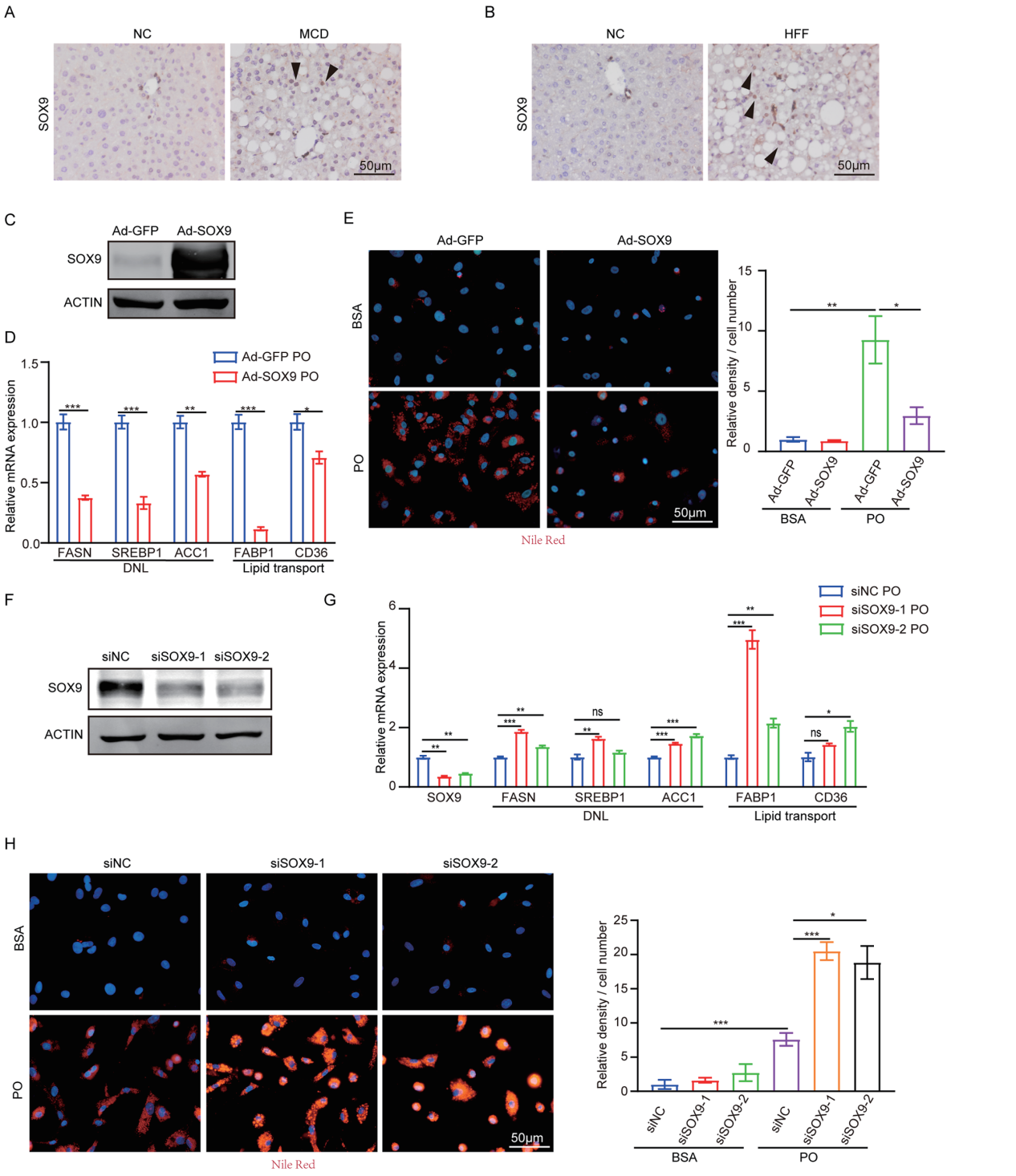

Fig. 1. SOX9 suppresses lipid accumulation in HepG2 cells. (A) Immunohistochemical staining of SOX9 in livers of C57BL/6J mice fed an MCD diet for eight weeks. (B) Immunohistochemical staining of SOX9 in livers of C57BL/6J mice fed an HFF diet for 12 weeks. (C) Western blot detecting the expression of SOX9 in HepG2 cells infected with Ad-GFP or Ad-SOX9. (D) mRNA levels of genes related to DNL (*FASN*, *SREBP1*, and *ACC1*) and lipid transport (*FABP1* and *CD36*) in HepG2 cells infected with Ad-GFP or Ad-SOX9 and treated with PO. (E) Nile Red staining in HepG2 cells infected with Ad-GFP or Ad-SOX9 and treated with BSA or PO. The right panel shows the relative Nile Red intensity per cell number, quantified by Image-Pro Plus (n = 4–7 fields per group). (F) Western blotting of SOX9 in HepG2 cells transfected with two siRNAs targeting SOX9 (siSOX9-1 or siSOX9-2). (G) Relative mRNA levels of genes related to DNL and lipid transport in HepG2 cells transfected with siRNAs targeting SOX9 and treated with PO. (H) Nile Red staining in PO- or BSA-treated HepG2 cells with SOX9 knockdown. The right panel shows the relative Nile Red intensity per cell number, quantified by Image-Pro Plus (n = 4–7 fields per group). All graphical data are presented as mean ± SEM. *$p < 0.05$, **$p < 0.01$, and ***$p < 0.001$. SOX9, sex-determining region Y-related high mobility group-box gene 9; PO, palmitic acid and oleic acid; FASN, fatty acid synthase; SREBP1, sterol regulatory element-binding protein 1; ACC1, acetyl-CoA carboxylase 1; FABP1, fatty acid binding protein 1; CD36, cluster of differentiation 36.

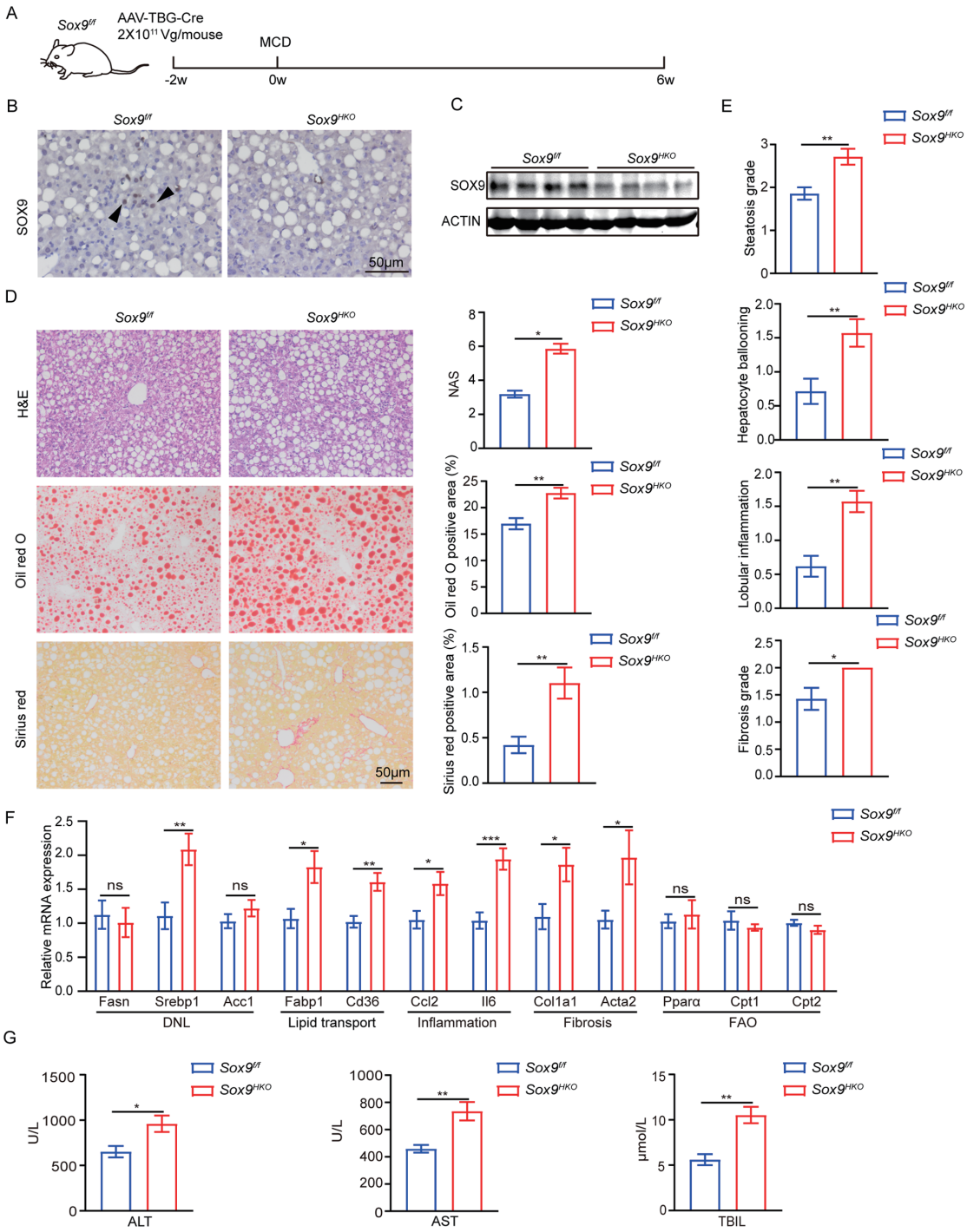

Fig. 2. Hepatocyte-specific deficiency of SOX9 aggravates hepatic steatosis. (A) Schematic of the experimental procedure for investigating the role of SOX9 in MCD-induced MASH in mice. (B) Immunohistochemical staining of SOX9 in livers of *SOX9*$^{f/f}$ and *SOX9*^{HKO} mice fed an MCD diet for six weeks. (C) Hepatic SOX9 protein levels in *SOX9*$^{f/f}$ and *SOX9*^{HKO} mice fed an MCD diet for six weeks. (D) Representative images of hematoxylin-eosin-stained, Oil Red O-stained, and Sirius Red-stained liver sections. Corresponding nonalcoholic fatty liver disease activity scores are provided. Lipids in Oil Red O-stained sections and collagen deposition in Sirius Red-stained sections are quantified using ImageJ. (E) Histological characterization of liver specimens from *SOX9*$^{f/f}$ and *SOX9*^{HKO} mice fed an MCD diet for six weeks. (F) Relative mRNA levels of genes related to DNL (*FASN*, *SREBP1*, and *ACC1*), lipid transport (*FABP1* and *CD36*), inflammation (*CCL2* and *IL6*), fibrosis (*COL1A1* and *ACTA2*), and FAO (*PPARα*, *CPT1*, and *CPT2*) in liver tissues from the indicated groups. (G) Serum levels of ALT, AST, and TBIL in *SOX9*$^{f/f}$ and *SOX9*^{HKO} mice fed an MCD diet for six weeks. All graphical data are presented as mean ± SEM. *$p < 0.05$, **$p < 0.01$, and ***$p < 0.001$. SOX9, sex-determining region Y-related high mobility group-box gene 9; MCD, methionine- and choline-deficient diet; FASN, fatty acid synthase; SREBP1, sterol regulatory element-binding protein 1; ACC1, acetyl-CoA carboxylase 1; FABP1, fatty acid binding protein 1; CD36, cluster of differentiation 36; CCL2, C-C motif chemokine ligand 2; IL6, interleukin 6; COL1A1, collagen type I alpha 1; ACTA2, actin alpha 2; PPARα, peroxisome proliferator-activated receptor alpha; CPT1, carnitine palmitoyltransferase 1; CPT2, carnitine palmitoyltransferase 2; ALT, alanine transaminase; AST, aspartate aminotransferase; TBIL, total bilirubin; TC, total cholesterol; TG, triglyceride.

overexpression reduced the expression of genes associated with DNL, lipid transport, inflammation, and fibrosis in liver tissues of MCD-fed mice (Supplementary Fig. 3F), as well as decreased serum ALT, AST, and TBIL levels (Supplementary Fig. 3G).

Overexpression of SOX9 in hepatocytes leads to therapeutic effects in HFF-induced MASH mice

To explore the therapeutic potential of SOX9 in MASH, we administered AAV-*SOX9* to mice that had been fed an HFF diet for six weeks, continuing the diet for an additional six weeks (Fig. 3A). Immunohistochemical staining and western blotting confirmed successful SOX9 overexpression in hepatocytes of AAV-*SOX9*-treated mice (Fig. 3B and C). Compared to controls, AAV-*SOX9*-treated mice exhibited significant reductions in steatosis, lipid accumulation, and fibrosis after 12 weeks on the HFF diet (Fig. 3D and E). Furthermore, AAV-*SOX9* treatment markedly downregulated the expression of genes involved in DNL, lipid transport, inflammation, and fibrosis in liver tissues (Fig. 3F). AAV-*SOX9* administration also improved insulin sensitivity, as demonstrated by glucose tolerance tests, and significantly reduced serum triglyceride and total cholesterol levels (Fig. 3G and H). Additionally, serum ALT and AST levels were lower in AAV-*SOX9*-treated mice compared to controls (Fig. 3I). Collectively, these findings suggest that AAV-mediated SOX9 overexpression in hepatocytes alleviates MASH progression.

SOX9 affects lipid metabolism, inflammation, and fibrosis in MCD-induced liver disease

To investigate the role of SOX9 in regulating lipid metabolism in MASH, we performed lipidomics and RNA-seq analyses on liver tissues from $SOX9^{HKO}$ and $SOX9^{f/f}$ mice after six weeks of MCD feeding. Lipidomic analysis identified 94 differentially expressed lipids between the $SOX9^{HKO}$ and $SOX9^{f/f}$ MCD groups, with 53 downregulated and 41 upregulated, underscoring SOX9's involvement in lipid metabolism regulation (Fig. 4A). The heatmap revealed substantial changes in lipid species across liver samples from $SOX9^{HKO}$ and $SOX9^{f/f}$ mice (Fig. 4B). Notably, several triacylglycerol and diacylglycerol species were upregulated in the livers of $SOX9^{HKO}$ mice, which are associated with the development and progression of MASLD (Fig. 4B).[28,29] Meanwhile, the liver content of cardiolipin and phosphatidylethanolamine, both essential for mitochondrial function and membrane integrity, decreased following specific knockout of SOX9 in hepatocytes.[30,31] These findings suggest that SOX9 regulates fatty liver disease through modulation of lipid composition. To further elucidate the mechanisms underlying these alterations, we performed Kyoto Encyclopedia of Genes and Genomes (KEGG) pathway analysis to assess lipid metabolism in relation to the differentially expressed lipids. This analysis highlighted key pathways related to lipid metabolism and autophagy affected by SOX9 depletion (Fig. 4C). Collectively, our lipidomics results demonstrate that SOX9 plays a critical role in hepatic lipid metabolism and composition.

RNA-seq analysis identified 169 DEGs in liver tissues from the two groups. Consistent with the lipidomics findings, Gene Ontology analysis revealed a strong association between these DEGs and biological processes involved in lipid metabolism (Fig. 4D). KEGG pathway analysis further highlighted that SOX9 deletion impacted several key pathways related to lipid metabolism, including fatty acid elongation, biosynthesis of unsaturated fatty acids, and the mTOR and AMPK pathways. Additionally, pathways linked to fibrosis, such as ECM-receptor interactions and the TGF-β signaling pathway, were altered (Fig. 4E). Disruption of SOX9 also affected other pathways, including the Hippo and Wnt signaling pathways, as previously reported.[32,33] Gene Set Enrichment Analysis indicated that SOX9 depletion exacerbated MCD-induced changes in lipid metabolism, inflammation, and fibrosis-related pathways (Fig. 4F and Supplementary Fig. 4A-B), reinforcing our earlier findings. Overall, these results suggest that SOX9 plays a central role in regulating MASH-related genes, lipids, and pathways in mice.

SOX9 activates the AMPK signaling pathway during MASH progression

In the KEGG pathway analysis (Fig. 4E), we identified the AMPK signaling pathway—a critical regulator of lipid metabolism—as being particularly enriched. Previous studies have demonstrated its essential role in MASH.[16,17] Our analysis of differentially expressed genes within the AMPK pathway revealed that 10 genes were downregulated in the $SOX9^{HKO}$ group (Fig. 5A). Western blotting confirmed that SOX9 overexpression enhanced AMPK activation, whereas its suppression inhibited AMPK activation in HepG2 cells (Fig. 5B and C). Similarly, in AML12 cells, SOX9 overexpression promoted AMPK activation (Supplementary Fig. 5A). These findings were corroborated in a MASH mouse model, where SOX9 knockout in hepatocytes suppressed AMPK signaling in the MCD model, while hepatocyte-specific overexpression of SOX9 activated the AMPK pathway in both MCD and HFF models (Fig. 5D-F).

To determine whether the protective effects of SOX9 during MASH progression are mediated through the AMPK pathway, we treated HepG2 cells with Compound C, an AMPK inhibitor (Fig. 5G). Inhibition of AMPK activation by Compound C abolished the lipid-reducing effects of Ad-SOX9 on PO-induced lipid accumulation, as evidenced by Nile Red staining (Fig. 5H). Additionally, qRT-PCR analysis showed that AMPK inhibition partially reversed the effects of SOX9 overexpression on lipid metabolism (Fig. 5I and Supplementary Fig. 5B). SIRT1, a known deacetylase, has been reported to activate the AMPK pathway.[34] We found that SOX9 overexpression upregulated both the mRNA and protein levels of SIRT1 (Fig. 5J-K), suggesting that SOX9 may regulate AMPK activation through transcriptional modulation of SIRT1 expression. However, the exact mechanisms remain to be fully elucidated. Together, these findings indicate that SOX9 overexpression mitigates lipotoxicity by activating the AMPK signaling pathway.

Discussion

SOX9 is a crucial regulator of embryogenesis and organ development.[35] In adult tissues, it marks progenitor cells and plays a key role in tissue regeneration following injury, contributing to the maintenance of organ homeostasis.[36,37] Genetic lineage tracing has shown that $SOX9^{+}$ hepatocytes actively proliferate and restore liver mass during regeneration.[7] Increased SOX9 expression has been observed in hepatocytes following CCl_4- and BDL-induced liver fibrosis,[38] suggesting that the expansion of $SOX9^{+}$ hepatocytes is a response to chronic liver injury. These findings highlight a protective role for SOX9 in restoring liver function during prolonged damage. In this study, we observed that SOX9 is upregulated in response to MASH, implying a similar protective function in this context.

SOX9, a key transcription factor, regulates multiple signaling pathways critical for cellular processes. It modulates the TGF-β and Hippo pathways, which are involved in cholangiocyte differentiation and bile duct morphogenesis.[39] Ad-

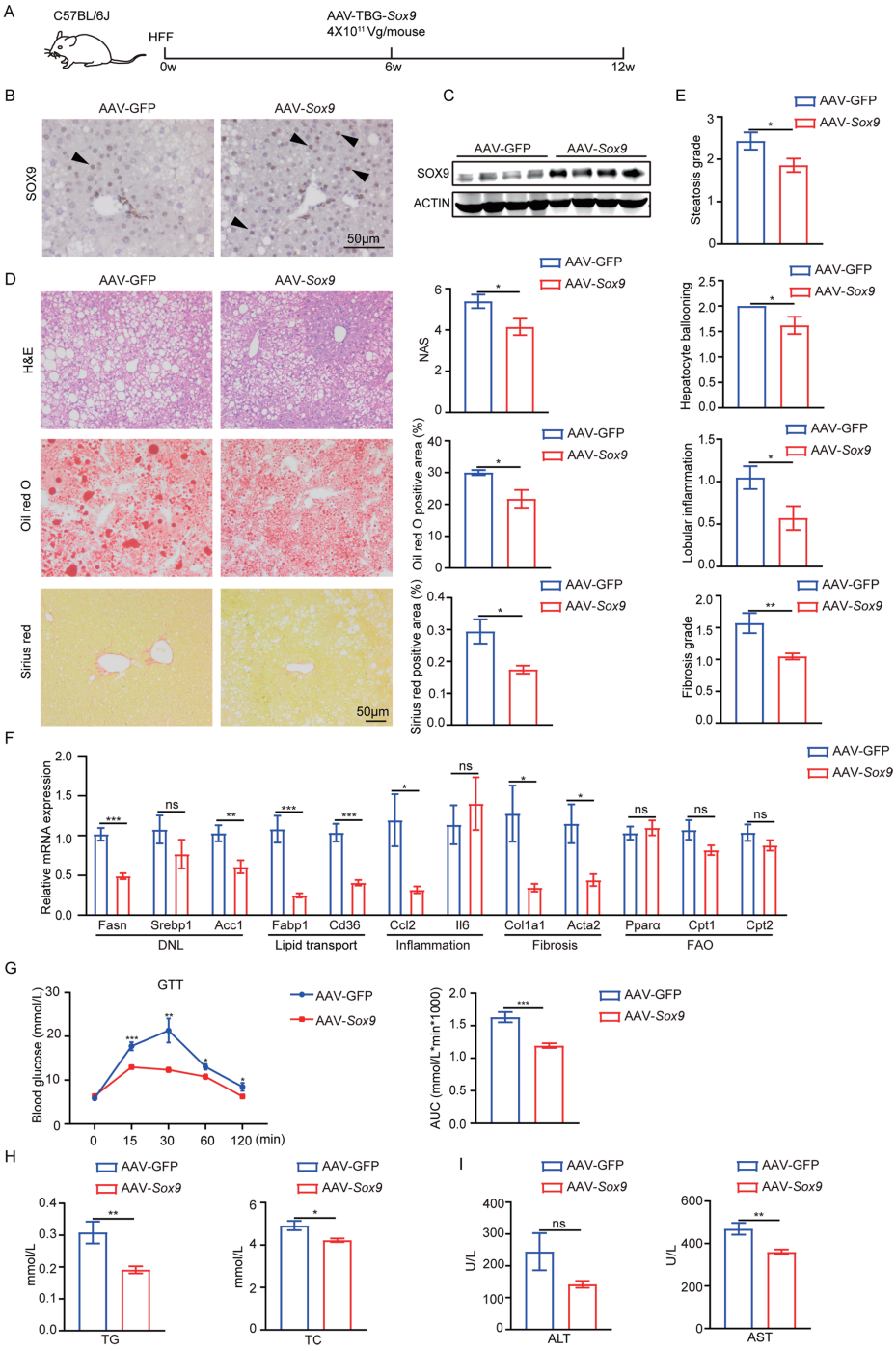

Fig. 3. SOX9 overexpression via adeno-associated virus attenuates hepatic steatosis in HFF-fed mice. (A) Schematic of the experimental procedure for testing the therapeutic effect of SOX9 in mice fed an HFF diet. (B) Immunohistochemical staining images of SOX9 expression in livers of HFF-fed mice injected with AAV-GFP or AAV-*SOX9*. (C) Hepatic SOX9 protein levels in HFF-fed mice injected with AAV-GFP or AAV-*SOX9*. (D) Representative hematoxylin-eosin-stained, Oil Red O-stained, and Sirius Red-stained liver sections. Corresponding nonalcoholic fatty liver disease activity scores are provided. Lipids in Oil Red O-stained sections and collagen deposition in Sirius Red-stained sections are quantified using ImageJ. (E) Histological characterization of liver specimens from HFF-fed mice injected with AAV-GFP or AAV-*SOX9*. (F) qRT-PCR analysis of transcript levels of genes related to DNL (*FASN*, *SREBP1*, and *ACC1*), lipid transport (*FABP1* and *CD36*), inflammation (*CCL2* and *IL6*), fibrosis (*COL1A1* and *ACTA2*), and FAO (*PPARα*, *CPT1*, and *CPT2*) in liver tissues from the indicated groups. (G) GTT assay of HFF-fed mice injected with AAV-GFP or AAV-*SOX9*. Corresponding areas under the curve values are provided. (H) Serum TG and TC concentrations in the indicated mouse groups. (I) Serum levels of ALT, AST, and TBIL in HFF-fed mice injected with AAV-GFP or AAV-*SOX9*. All graphical data are presented as mean ± SEM. *$p < 0.05$, **$p < 0.01$, and ***$p < 0.001$. SOX9, sex-determining region Y-related high mobility group-box gene 9; HFF, high-fat high-fructose; FASN, fatty acid synthase; SREBP1, sterol regulatory element-binding protein 1; ACC1, acetyl-CoA carboxylase 1; FABP1, fatty acid binding protein 1; CD36, cluster of differentiation 36; CCL2, C-C motif chemokine ligand 2; IL6, interleukin 6; COL1A1, collagen type I alpha 1; ACTA2, actin alpha 2; PPARα, peroxisome proliferator-activated receptor alpha; CPT1, carnitine palmitoyltransferase 1; CPT2, carnitine palmitoyltransferase 2; ALT, alanine transaminase; AST, aspartate aminotransferase; TBIL, total bilirubin; TC, total cholesterol; TG, triglyceride.

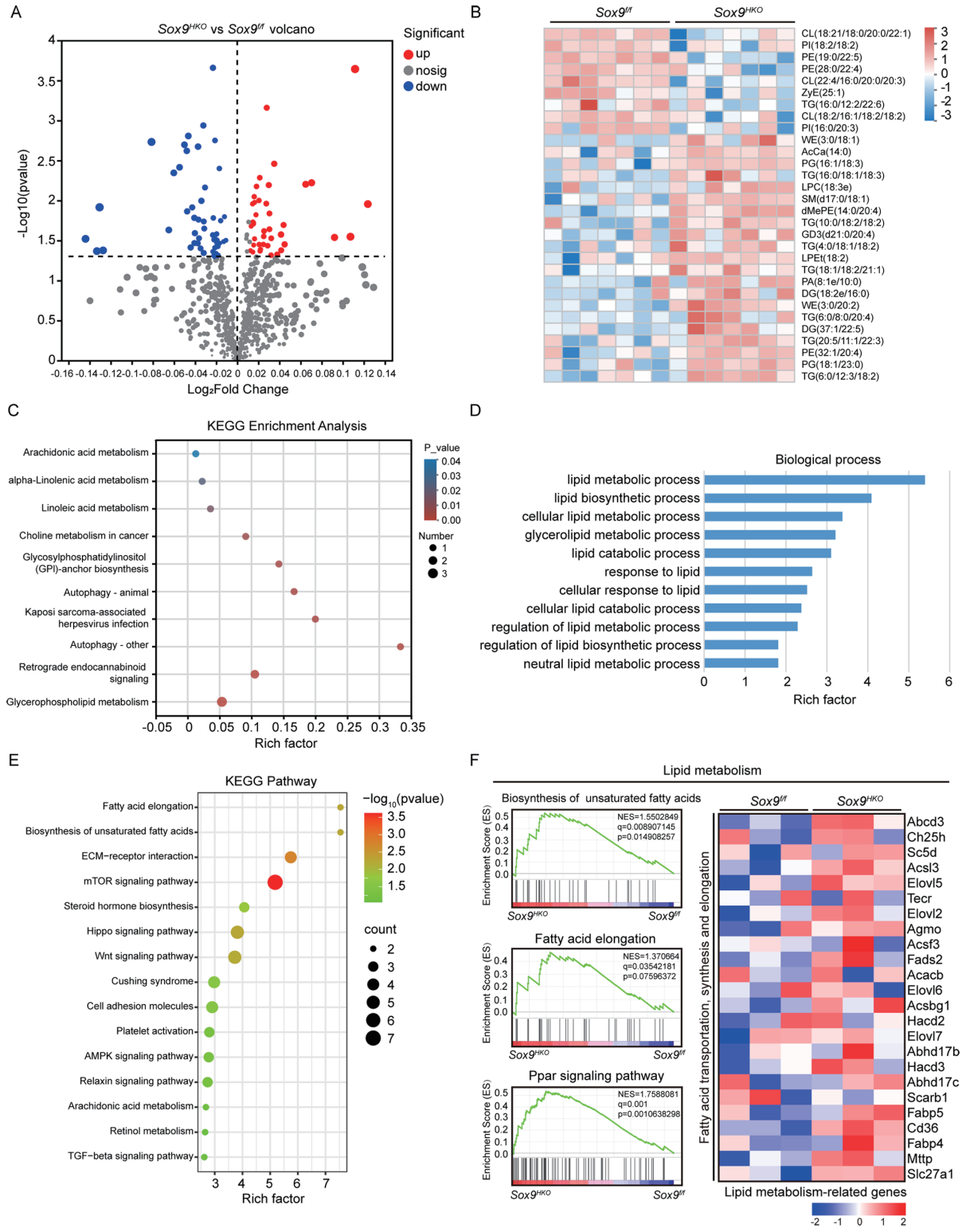

Fig. 4. Hepatocyte SOX9 influences lipid composition in the liver. (A) Volcano plot of differential metabolites in the livers of *SOX9*^{HKO} MCD and *SOX9*$^{f/f}$ MCD mice. (B) Heatmap of lipid levels in the livers of *SOX9*^{HKO} MCD and *SOX9*$^{f/f}$ MCD mice. (C) KEGG analysis of lipid metabolism related to differential lipids between *SOX9*^{HKO} MCD and *SOX9*$^{f/f}$ MCD mice. (D) GO analysis of DEGs between *SOX9*^{HKO} and *SOX9*$^{f/f}$ mice based on RNA-Seq data from liver tissues. (E) KEGG enrichment analysis of the RNA-seq data showing significantly altered pathways. (F) Gene Set Enrichment Analysis and heatmap illustrating the expression levels of pathways and genes associated with lipid metabolism in the livers of *SOX9*$^{f/f}$ and *SOX9*^{HKO} mice. SOX9, sex-determining region Y-related high mobility group-box gene 9; KEGG, Kyoto Encyclopedia of Genes and Genomes; GO, Gene Ontology.

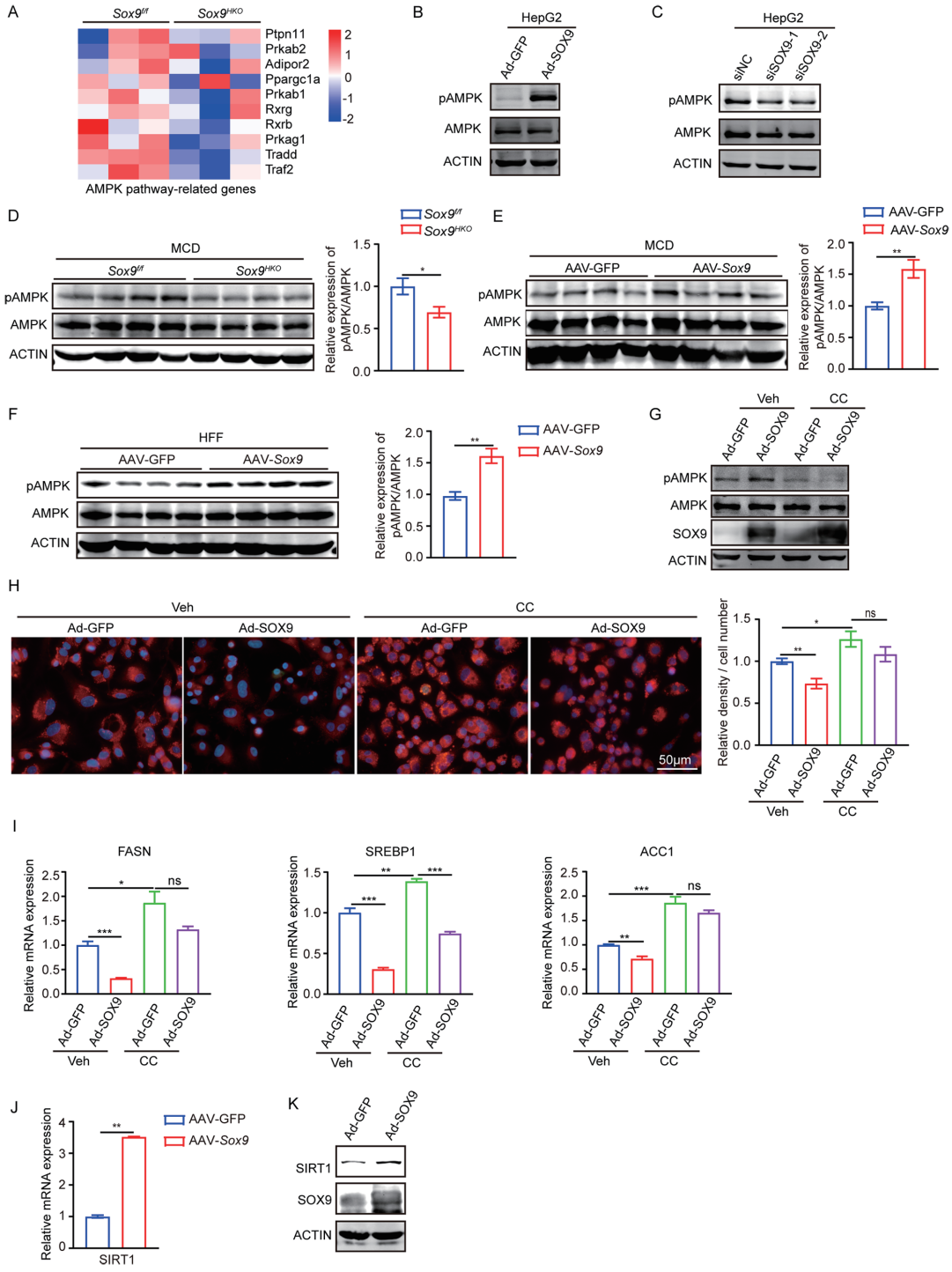

Fig. 5. SOX9 activates the AMPK pathway during the progression of MASH. (A) Heatmap showing changes in the levels of AMPK pathway-related gene expression. (B) Protein levels of total and phosphorylated AMPK in HepG2 cells infected with Ad-GFP or Ad-SOX9. (C) Protein levels of total and phosphorylated AMPK in HepG2 cells transfected with two siRNAs targeting SOX9 (siSOX9-1 or siSOX9-2) or the corresponding control. (D and E) Phosphorylated and total protein levels of AMPK in livers of MCD-fed *SOX9*$^{f/f}$ and *SOX9*^{HKO} mice (D) or MCD-fed AAV-GFP- or AAV-*SOX9*-administered mice (E). (F) Phosphorylated and total protein levels of AMPK in livers of HFF-fed mice administered with AAV-GFP or AAV-*SOX9*. (G) Phosphorylated and total AMPK protein levels in HepG2 cells infected with Ad-SOX9 or Ad-GFP. Cells were subsequently challenged with PO and treated with CC (10 μM) or vehicle for 24 h. (H) The extent of lipid deposition in HepG2 cells was assessed by Nile Red staining. HepG2 cells were infected with Ad-SOX9 or Ad-GFP, then challenged with PO and treated with CC (10 μM) or vehicle for 24 h. The density of Nile Red staining per cell number was quantified by Image-Pro Plus. n = 4–7 fields per group. (I) Relative mRNA expression of FASN, SREBP1, and ACC1 in HepG2 cells under CC treatment. (J and K) mRNA and protein levels of SIRT1 in HepG2 cells infected with Ad-GFP or Ad-SOX9. All graphical data are presented as mean ± SEM. *p<0.05, **p<0.01, and ***p<0.001. SOX9, sex-determining region Y-related high mobility group-box gene 9; AMPK, AMP-activated protein kinase; MCD, methionine- and choline-deficient diet; HFF, high-fat high-fructose; CC, compound C.

ditionally, SOX9 enhances hepatocellular carcinoma (HCC) stemness by activating the Wnt pathway.[40] Both the Hippo and Wnt pathways are implicated in the progression of MASLD.[41,42] Our RNA-seq data corroborate these findings, emphasizing the regulatory role of SOX9 in these pathways. Previous studies have also identified SOX9 as a metabolic regulator in various cell types.[10,11] In this study, we reveal that SOX9 functions as a novel suppressor of MASH in hepatocytes.

Our findings demonstrate that SOX9 regulates lipid metabolism, inflammation, and fibrosis processes during MASH progression, influencing key metabolic pathways such as AMPK and mTOR. These pathways are pivotal in maintaining cellular metabolism and energy homeostasis.[43] This study highlights SOX9's critical role in cellular lipid metabolism and its potential as a therapeutic target for MASH. Given that MASH is a leading cause of non-cirrhotic HCC,[44] and previous studies suggest that SOX9 exacerbates HCC malignancy and promotes cancer progression,[8,9] we propose a dual role for SOX9. It may slow disease progression during early liver disease stages, such as MASH, but contribute to disease advancement in later stages, such as HCC. Therapeutic strategies targeting SOX9 should therefore consider the disease stage to optimize outcomes.

AMPK serves as a critical energy sensor that maintains cellular energy balance by regulating metabolic pathways.[12] In the liver, AMPK activation inhibits DNL and promotes fatty acid oxidation through the phosphorylation of acetyl-CoA carboxylase, thereby alleviating MASLD.[45] Key upstream activators of the AMPK pathway include CAMKK2, liver kinase B1, and TAK1.[46] Through RNA-seq data analysis and *in vivo* and *in vitro* experiments, we identified SOX9 as a regulator of the AMPK pathway. Previous research has shown that AMPK inhibition downregulates SOX9 expression in chondrocytes *in vitro*.[47] Our findings indicate a reciprocal regulatory relationship, as SOX9 was observed to activate AMPK. Notably, SOX9 overexpression led to increased expression of SIRT1, a deacetylase that activates AMPK by deacetylating and promoting the cytosolic localization of liver kinase B1.[34] This suggests that SOX9 influences AMPK activation through the modulation of SIRT1 levels. However, the precise regulatory mechanisms remain to be elucidated.

Conclusions

Our results demonstrate that SOX9 overexpression reduces MASH progression by promoting AMPK activation. These findings position SOX9 as a promising therapeutic target for treating MASH.

Funding

This study was supported by the National Natural Science Foundation of China (grant numbers 81900514, 82072641, and 82030021).

Conflict of interest

The authors declare no conflicts of interest related to this publication.

Author contributions

WX, XZ and KD conceived the research project. JD, KD, SL, FC, RH, BX performed the research project; JD analyzed experimental data, interpreted the results. JD and KD drafted the manuscript; WX and XZ reviewed the manuscript. All authors have read and approved the final version and the publication of the manuscript.

Ethical statement

All animal procedures were performed in compliance with the National Institutes of Health Guide for the Care and Use of Laboratory Animals and were approved by the Scientific Investigation Board of Naval Medical University (Project NO. 81900514). Procedures involving the collection and use of human samples were ethically approved by the Ethics Committee of Naval Medical University (Project NO. 81900514) and adhered to the principles outlined in the Declaration of Helsinki. All participants provided written informed consent prior to sample collection.

Data sharing statement

The RNA-seq dataset derived from liver tissues from *SOX-9^{HKO}* and *SOX9$^{f/f}$* mice has been deposited in the NCBI Gene Expression Omnibus under accession number GSE237075. Transcriptomic data from liver samples of MASLD and control patients were retrieved from the Gene Expression Omnibus, under accession ID GSE135251. The lipidomic analysis data used in support of the findings of this study are available from the corresponding author at weifenxie@smmu.edu.cn upon request.

References

[1] Patel AH, Peddu D, Amin S, Elsaid MI, Minacapelli CD, Chandler TM, *et al*. Nonalcoholic Fatty Liver Disease in Lean/Nonobese and Obese Individuals: A Comprehensive Review on Prevalence, Pathogenesis, Clinical Outcomes, and Treatment. J Clin Transl Hepatol 2023;11(2):502–515. doi:10.14218/JCTH.2022.00204, PMID:36643037.
[2] Polyzos SA, Kountouras J, Mantzoros CS. Obesity and nonalcoholic fatty liver disease: From pathophysiology to therapeutics. Metabolism 2019;92:82–97. doi:10.1016/j.metabol.2018.11.014, PMID:30502373.
[3] Cusi K, Isaacs S, Barb D, Basu R, Caprio S, Garvey WT, *et al*. American Association of Clinical Endocrinology Clinical Practice Guideline for the Diagnosis and Management of Nonalcoholic Fatty Liver Disease in Primary Care and Endocrinology Clinical Settings: Co-Sponsored by the American Association for the Study of Liver Diseases (AASLD). Endocr Pract 2022;28(5):528–562. doi:10.1016/j.eprac.2022.03.010, PMID:35569886.
[4] Friedman SL, Neuschwander-Tetri BA, Rinella M, Sanyal AJ. Mechanisms of NAFLD development and therapeutic strategies. Nat Med 2018;24(7):908–922. doi:10.1038/s41591-018-0104-9, PMID:29967350.
[5] Ming Z, Vining B, Bagheri-Fam S, Harley V. SOX9 in organogenesis: shared and unique transcriptional functions. Cell Mol Life Sci 2022;79(10):522. doi:10.1007/s00018-022-04543-4, PMID:36114905.
[6] Han X, Wang Y, Pu W, Huang X, Qiu L, Li Y, *et al*. Lineage Tracing Reveals the Bipotency of SOX9(+) Hepatocytes during Liver Regeneration. Stem Cell Reports 2019;12(3):624–638. doi:10.1016/j.stemcr.2019.01.010, PMID:30773487.
[7] Font-Burgada J, Shalapour S, Ramaswamy S, Hsueh B, Rossell D, Umemura A, *et al*. Hybrid Periportal Hepatocytes Regenerate the Injured Liver without Giving Rise to Cancer. Cell 2015;162(4):766–779. doi:10.1016/j.cell.2015.07.026, PMID:26276631.
[8] Ren Z, Chen Y, Shi L, Shao F, Sun Y, Ge J, *et al*. Sox9/CXCL5 axis facilitates tumour cell growth and invasion in hepatocellular carcinoma. FEBS J 2022;289(12):3535–3549. doi:10.1111/febs.16357, PMID:35038357.
[9] Liu C, Liu L, Chen X, Cheng J, Zhang H, Shen J, *et al*. Sox9 regulates self-renewal and tumorigenicity by promoting symmetrical cell division of cancer stem cells in hepatocellular carcinoma. Hepatology 2016;64(1):117–129. doi:10.1002/hep.28509, PMID:26910875.
[10] Wang Y, Sul HS. Pref-1 regulates mesenchymal cell commitment and differentiation through Sox9. Cell Metab 2009;9(3):287–302. doi:10.1016/j.cmet.2009.01.013, PMID:19254573.
[11] van Gastel N, Stegen S, Eelen G, Schoors S, Carlier A, Daniëls VW, *et al*. Lipid availability determines fate of skeletal progenitor cells via SOX9. Nature 2020;579(7797):111–117. doi:10.1038/s41586-020-2050-1, PMID:32103177.
[12] Wang Q, Liu S, Zhai A, Zhang B, Tian G. AMPK-Mediated Regulation of Lipid Metabolism by Phosphorylation. Biol Pharm Bull 2018;41(7):985–993. doi:10.1248/bpb.b17-00724, PMID:29709897.
[13] Lin SC, Hardie DG. AMPK: Sensing Glucose as well as Cellular Energy Status. Cell Metab 2018;27(2):299–313. doi:10.1016/j.cmet.2017.10.009, PMID:29153408.
[14] Mottillo EP, Desjardins EM, Crane JD, Smith BK, Green AE, Ducommun S,

et al. Lack of Adipocyte AMPK Exacerbates Insulin Resistance and Hepatic Steatosis through Brown and Beige Adipose Tissue Function. Cell Metab 2016;24(1):118–129. doi:10.1016/j.cmet.2016.06.006, PMID:27411013.
[15] Lan T, Yu Y, Zhang J, Li H, Weng Q, Jiang S, *et al*. Cordycepin Ameliorates Nonalcoholic Steatohepatitis by Activation of the AMP-Activated Protein Kinase Signaling Pathway. Hepatology 2021;74(2):686–703. doi:10.1002/hep.31749, PMID:33576035.
[16] Zhao P, Sun X, Chaggan C, Liao Z, In Wong K, He F, *et al*. An AMPK-caspase-6 axis controls liver damage in nonalcoholic steatohepatitis. Science 2020;367(6478):652–660. doi:10.1126/science.aay0542, PMID:32029622.
[17] Garcia D, Hellberg K, Chaix A, Wallace M, Herzig S, Badur MG, *et al*. Genetic Liver-Specific AMPK Activation Protects against Diet-Induced Obesity and NAFLD. Cell Rep 2019;26(1):192–208.e6. doi:10.1016/j.celrep.2018.12.036, PMID:30605676.
[18] Yin C, Lin Y, Zhang X, Chen YX, Zeng X, Yue HY, *et al*. Differentiation therapy of hepatocellular carcinoma in mice with recombinant adenovirus carrying hepatocyte nuclear factor-4alpha gene. Hepatology 2008;48(5):1528–1539. doi:10.1002/hep.22510, PMID:18925631.
[19] Chomczynski P, Sacchi N. Single-step method of RNA isolation by acid guanidinium thiocyanate-phenol-chloroform extraction. Anal Biochem 1987;162(1):156–159. doi:10.1006/abio.1987.9999, PMID:2440339.
[20] Livak KJ, Schmittgen TD. Analysis of relative gene expression data using real-time quantitative PCR and the 2(-Delta Delta C(T)) Method. Methods 2001;25(4):402–408. doi:10.1006/meth.2001.1262, PMID:11846609.
[21] Mahmood T, Yang PC. Western blot: technique, theory, and trouble shooting. N Am J Med Sci 2012;4(9):429–434. doi:10.4103/1947-2714.100998, PMID:23050259.
[22] Conesa A, Madrigal P, Tarazona S, Gomez-Cabrero D, Cervera A, McPherson A, *et al*. A survey of best practices for RNA-seq data analysis. Genome Biol 2016;17:13. doi:10.1186/s13059-016-0881-8, PMID:26813401.
[23] Xia QS, Wu F, Wu WB, Dong H, Huang ZY, Xu L, *et al*. Berberine reduces hepatic ceramide levels to improve insulin resistance in HFD-fed mice by inhibiting HIF-2α. Biomed Pharmacother 2022;150:112955. doi:10.1016/j.biopha.2022.112955, PMID:35429745.
[24] Kleiner DE, Brunt EM, Van Natta M, Behling C, Contos MJ, Cummings OW, *et al*. Design and validation of a histological scoring system for nonalcoholic fatty liver disease. Hepatology 2005;41(6):1313–1321. doi:10.1002/hep.20701, PMID:15915461.
[25] Schindelin J, Arganda-Carreras I, Frise E, Kaynig V, Longair M, Pietzsch T, *et al*. Fiji: an open-source platform for biological-image analysis. Nat Methods 2012;9(7):676–682. doi:10.1038/nmeth.2019, PMID:22743772.
[26] Ramos-Vara JA. Technical aspects of immunohistochemistry. Vet Pathol 2005;42(4):405–426. doi:10.1354/vp.42-4-405, PMID:16006601.
[27] Greenspan P, Mayer EP, Fowler SD. Nile red: a selective fluorescent stain for intracellular lipid droplets. J Cell Biol 1985;100(3):965–973. doi:10.1083/jcb.100.3.965, PMID:3972906.
[28] Semova I, Biddinger SB. Triglycerides in Nonalcoholic Fatty Liver Disease: Guilty Until Proven Innocent. Trends Pharmacol Sci 2021;42(3):183–190. doi:10.1016/j.tips.2020.12.001, PMID:33468321.
[29] Gorden DL, Ivanova PT, Myers DS, McIntyre JO, VanSaun MN, Wright JK, *et al*. Increased diacylglycerols characterize hepatic lipid changes in progression of human nonalcoholic fatty liver disease; comparison to a murine model. PLoS One 2011;6(8):e22775. doi:10.1371/journal.pone.0022775, PMID:21857953.
[30] Kiebish MA, Bell R, Yang K, Phan T, Zhao Z, Ames W, *et al*. Dynamic simulation of cardiolipin remodeling: greasing the wheels for an interpretative approach to lipidomics. J Lipid Res 2010;51(8):2153–2170. doi:10.1194/jlr.M004796, PMID:20410019.
[31] Rong S, Xia M, Vale G, Wang S, Kim CW, Li S, *et al*. DGAT2 inhibition blocks SREBP-1 cleavage and improves hepatic steatosis by increasing phosphatidylethanolamine in the ER. Cell Metab 2024;36(3):617–629.e7. doi:10.1016/j.cmet.2024.01.011, PMID:38340721.
[32] Liu Y, Zhuo S, Zhou Y, Ma L, Sun Z, Wu X, *et al*. Yap-Sox9 signaling determines hepatocyte plasticity and lineage-specific hepatocarcinogenesis. J Hepatol 2022;76(3):652–664. doi:10.1016/j.jhep.2021.11.010, PMID:34793870.
[33] Huang JQ, Wei FK, Xu XL, Ye SX, Song JW, Ding PK, *et al*. SOX9 drives the epithelial-mesenchymal transition in non-small-cell lung cancer through the Wnt/β-catenin pathway. J Transl Med 2019;17(1):143. doi:10.1186/s12967-019-1895-2, PMID:31060551.
[34] Lan F, Cacicedo JM, Ruderman N, Ido Y. SIRT1 modulation of the acetylation status, cytosolic localization, and activity of LKB1. Possible role in AMP-activated protein kinase activation. J Biol Chem 2008;283(41):27628–27635. doi:10.1074/jbc.M805711200, PMID:18687677.
[35] Jo A, Denduluri S, Zhang B, Wang Z, Yin L, Yan Z, *et al*. The versatile functions of Sox9 in development, stem cells, and human diseases. Genes Dis 2014;1(2):149–161. doi:10.1016/j.gendis.2014.09.004, PMID:25685828.
[36] Furuyama K, Kawaguchi Y, Akiyama H, Horiguchi M, Kodama S, Kuhara T, *et al*. Continuous cell supply from a Sox9-expressing progenitor zone in adult liver, exocrine pancreas and intestine. Nat Genet 2011;43(1):34–41. doi:10.1038/ng.722, PMID:21113154.
[37] Kawaguchi Y. Sox9 and programming of liver and pancreatic progenitors. J Clin Invest 2013;123(5):1881–1886. doi:10.1172/JCI66022, PMID:23635786.
[38] Athwal VS, Pritchett J, Llewellyn J, Martin K, Camacho E, Raza SM, *et al*. SOX9 predicts progression toward cirrhosis in patients while its loss protects against liver fibrosis. EMBO Mol Med 2017;9(12):1696–1710. doi:10.15252/emmm.201707860, PMID:29109128.
[39] Poncy A, Antoniou A, Cordi S, Pierreux CE, Jacquemin P, Lemaigre FP. Transcription factors SOX4 and SOX9 cooperatively control development of bile ducts. Dev Biol 2015;404(2):136–148. doi:10.1016/j.ydbio.2015.05.012, PMID:26033091.
[40] Leung CO, Mak WN, Kai AK, Chan KS, Lee TK, Ng IO, *et al*. Sox9 confers stemness properties in hepatocellular carcinoma through Frizzled-7 mediated Wnt/β-catenin signaling. Oncotarget 2016;7(20):29371–29386. doi:10.18632/oncotarget.8835, PMID:27105493.
[41] Jeong SH, Kim HB, Kim MC, Lee JM, Lee JH, Kim JH, *et al*. Hippo-mediated suppression of IRS2/AKT signaling prevents hepatic steatosis and liver cancer. J Clin Invest 2018;128(3):1010–1025. doi:10.1172/JCI95802, PMID:29400692.
[42] Shree Harini K, Ezhilarasan D. Wnt/beta-catenin signaling and its modulators in nonalcoholic fatty liver diseases. Hepatobiliary Pancreat Dis Int 2023;22(4):333–345. doi:10.1016/j.hbpd.2022.10.003, PMID:36448560.
[43] Inoki K, Kim J, Guan KL. AMPK and mTOR in cellular energy homeostasis and drug targets. Annu Rev Pharmacol Toxicol 2012;52:381–400. doi:10.1146/annurev-pharmtox-010611-134537, PMID:22017684.
[44] Stine JG, Wentworth BJ, Zimmet A, Rinella ME, Loomba R, Caldwell SH, *et al*. Systematic review with meta-analysis: risk of hepatocellular carcinoma in non-alcoholic steatohepatitis without cirrhosis compared to other liver diseases. Aliment Pharmacol Ther 2018;48(7):696–703. doi:10.1111/apt.14937, PMID:30136293.
[45] Smith BK, Marcinko K, Desjardins EM, Lally JS, Ford RJ, Steinberg GR. Treatment of nonalcoholic fatty liver disease: role of AMPK. Am J Physiol Endocrinol Metab 2016;311(4):E730–E740. doi:10.1152/ajpendo.00225.2016, PMID:27577854.
[46] Herzig S, Shaw RJ. AMPK: guardian of metabolism and mitochondrial homeostasis. Nat Rev Mol Cell Biol 2018;19(2):121–135. doi:10.1038/nrm.2017.95, PMID:28974774.
[47] Liu J, Zuo Q, Li Z, Chen J, Liu F. Trelagliptin ameliorates IL-1β-impaired chondrocyte function via the AMPK/SOX-9 pathway. Mol Immunol 2021;140:70–76. doi:10.1016/j.molimm.2021.09.009, PMID:34666245.